Int. Studiengang Bionik B.Sc.
Hochschule Bremen

Internship report

Hydrodynamic study of Lac Bay, Bonaire – mapping the connected fluxes

Sophie K. Grützmacher

Student number: 5002825

Supervisor: Dr. Lucy Gwen Gillis, ZMT Bremen

and

Sabine Engel, STINAPA Bonaire

Submission date: 30th January 2020

Cover photo:

Downward-facing Nortek ADCP deployment in the backwater channels and lagoons

Contents

List of Figures

1. Abstract

The since 2003 protected RAMSAR site Lac Bay in the southeast of Bonaire is under stress due to degrading mangroves (mostly *Rhizophora mangle* and *Avicennia germanis*), sedimentation and salinization in the northern areas because of overgrazing, a southwards expanding mangrove cover and insufficient water exchange throughout the bay. 2010 volunteers started opening up channels and increasing the water income, however, there are little to no studies regarding the hydrodynamics in the backwater areas. In order to understand the hydrodynamics of Lac Bay and develop recommondations for the management of these channels the three-dimensional velocity was measured using Acoustic Doppler Current Profilers (ADCP) in four locations in the open parts of the bay and six selected sites within the lagoons and backwater channels.

The mostly north to northeast heading incoming currents and mostly southeast to southwest moving outgoing currents in the channels and lagoons often matched the expectations on most testing sites but with a bandwidth increasing with distance to the open bay while the magnitude is decreasing. The sheet flow system showed, depending on the measurement position and the surrounding lagoons serving as buffer storage, great delays and adjustment periods to the tidal changes up to 8 hours resulting in poor water exchange during little tides. A recommendation for a new to open channel from Kuki Perdi northwards into the backwater area was given based on the directions and spatial magnitude distribution of the incoming tide.

Keywords: mangrove health, *Rhizophora*, *Avicennia*, salinization, water exchange, tidal currents

2. Introduction

The island Bonaire 80 km before the venezuelan cost is a part of the Netherlands. It is 38.6 km long and 4.8 – 8 km wide (*Tourism Bonaire*). Lac Bay covers approximately 7 km^2 in the southeast of Bonaire and contains three ecologically and hydro-dynamically relevant connected ecosystems, coral reefs, seagrass meadows and mangrove forests. The coral reef acts as barrier limiting and directing the water exchange between the bay and the open sea (Figure 2.1). The seagrass meadows (mainly *Thalassia testudium)* and algal communities (mostly *Halimedae*) (Engel 2008) convert the nutrients from the mangrove forest into food for the local fauna and provide habitat for various fish species as well as the endangered queen conch (*Strombus gigas*) and the green turtle (*Chelonia mydas*). The seagrass meadows further reduce hydrodynamic energy. The mangrove forests provide nutrients but also a fish nursery and breeding habitats for birds. Lac Bay is a protected RAMSAR site since 2003. The functionality of this important ecological area is not only closely linked to the health of the mangrove forest, seagrass meadow and coral reefs but also to the sufficient water circulation in the bay, especially the backwater area. (Davaasuren and Meesters 2012)

Overgrazing by livestock in the terrestrial area behind the mangrove forests is increasing the sedimentation of the northern bay area. This increased sedimentation has meant that the back part of the mangrove forest close to the land has had reduced circulation of fresh seawater and the area has become hypersaline (Wosten 2013). The mangroves, mainly red mangroves (*Rhizophora mangle*) and black mangroves (*Avicennia germanis*), are degraded in many areas, creating lagoon areas which are filling further with terrigenous sediment (Debrot et al. 2010). Approximately 40 - 44 % of the remaining mangrove cover is unhealthy, especially in the backwater areas were lagoons and channels have been overgrown by southward expanding mangroves. (Davaasuren and Meesters 2012)

Over the last decade an estimated 0.6 km^2 of the 1.5 km^2 mangrove cover have died in the backwater, increasing the expansion of hypersalinine areas with little or no biodiversity. Meanwhile, around 0.6 km^2 of mangroves have newly settled towards the open bay (Figure 2.1, Figure 2.2), replacing the ecologically and hydro-dynamically valuable seagrass meadows (Wosten 2013). Thus altering the hydrodynamics of the entire bay. Since 2010 a team of volunteers guided by STINAPA scientific researcher Ms. Engel began to open former, grown shut mangrove channels and maintain reopened channels (see overview Figure 2.1) in order to facilitate the water flow into the backwater area and reconnect those water bodies with the open bay. This should increase the health of the mangroves and allowing them to continue to serve as a nursery area for fish, a nutrient source for seagrass meadows and as breeding and feeding ground for birds again(Wosten 2013).

As indicated Lac Bay is a dynamic area, where changes in the distribution of these important dynamically relevant connected ecosystems can affect the health of the whole Bay. However, although several studies has concentrated on the changes in ecosystem functioning (Debrot 2012), there are little to no studies regarding the hydrodynamics of this area. Consequently, the following study is a first attempt to further understand the connected fluxes in Lac Bay. The three-dimensional velocity over the tide cycles was measured with Acoustic Doppler Current Profilers (ADCP) in four locations in the open parts of the bay and six selected sites within the backwater channels to develop recommendations for optimized channels.

2.1. Current state of science

Lay Bay itself is approximately 1 - 4 m deep and is exposed to a North-eastern wind. Moorsel and Meijer (1993) created a bathymetric map, showing a with channel around 4 m to 5 m deep leading from the middle of the bay towards the narrow, ca. 8 m deep exit to the open ocean. This channel was identified as suitable for ADCP measurements, because the main water exchange would most likely occur along this channel. Additionally for logistical reasons, the ADCP has a height and a blanking space which add up to ca. 0.7 m which cannot be measured, which makes especially the here taken upward looking measurements from the bottom unsuited for measuring the deeper currents in shallow areas. Other than that, Moorsel and Meijer (1993) provides a map with the tidal delays and tidal ranges throughout the bay as well as a map showing roughly the water flows in parts of Lac Bay (Figure 2.2), whereby the tide as well as the methodology is not specified, stating only the currents were "determined by tracking particles along a 1 m long folding rule held in the water, the passage duration being measured with an underwater stopwatch. The flow velocity was calculated from this. Combined with tide measurements, temperature profiles, salinity and visual observations of flow direction and aerial photos, a global flow chart of the area was compiled from this".

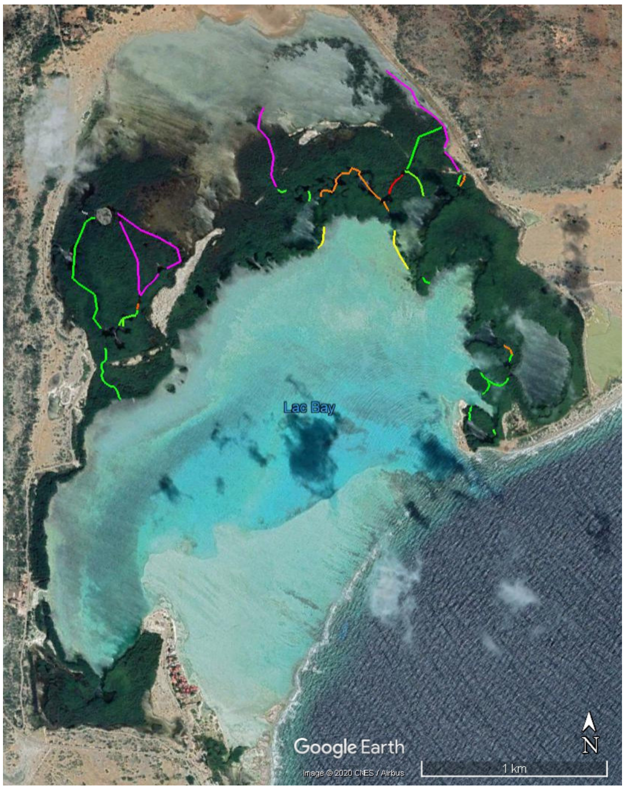

Figure 2.1: Channels throughout the mangroves of Lac Bay: green: open, yellow: border maintenance, orange: maintenance, red: current workings, purple: planned, grey: mostly enclosed. Satellite picture from 12.2018. Altered from Engel (2019)

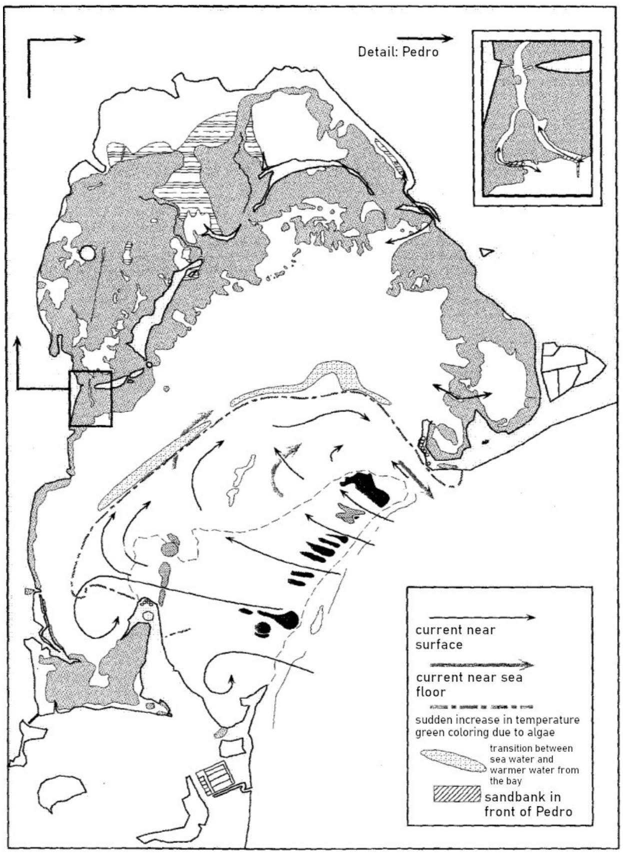

Figure 2.2: Current state of knowledge about the waterexchange in Lac Bay and distributrion of the mangrove cover 1993. Altered from Moorsel and Meijer (1993)

3. Materials and methods

Before the study the functionality of all three ADCPs were tested and the compasses were calibrated according to RD Instruments (2001) and Nortek AS (2018), taking the metal rebars at the Sentinel Workhorse ADCPs into consideration. With each deployment and retrieval the water depth from surface to the ground as well as from the surface and from the ground to the transducer of the ADCP was measured with a reel (Table A.1,

to take the body of the ADCP were no measurements are possible into consideration when transforming from cells to absolute range.

3.1. Open bay

Two WorkHorse Sentinel Acoustic Doppler Current Profiler (ADCPs) from RD Instruments (San Diego, USA, later Teledyne RD Instruments, Poway, USA) were used to profile in total four locations in the open area of Lac Bay (Figure 3.1). One ADCP was used as a reference point which stayed constant during all deployments. The other ADCP was moved between the remaining three locations on a weekly basis so each deployment would measure approximately 5 or 6 full tidal cycles. The ADCPs were deployed upward-facing at the sea floor. Sandy spots were chosen at each location in order to avoid destroying the surrounding seagrass patches. The ADCPs were anchored in place with the head as close to the sea floor as possible to reduce the part of the watercolumn that was not measured. Additionally, the ADCPs were pinned down with four 1 m steel rebars which were bent in the center, here hooks were attached to the bottom part of the ADCP.

All deployments were programmed identically in order to insure comparability. The planning of the deployments were completed with the software WinSC Application Version 1.29 by RD Instruments (San Diego, USA). The frequency was set to 1200 kHz, the ensemble interval was chosen to be 1 h, with 60 water pings per ensemble. The salinity was fixed at 40 ppt, the temperature at 30 °C. Depth cell size was set to 0.2 m, with a blanking space of 0.6 m which resulted in the first cell range being at 0.7 m. All cell ranges are referring to the middle of each cell, meaning, the first cell covered a range from 0.6 - 0.8 m. The last cell range was set to 5.3 m which resulted in 24 depth cells in total. Resulting from these setups were a standard deviation of 28.7 $\mathrm{mm\,s^{-1}}$, the ambiguity velocity was 1.75 $\mathrm{m\,s^{-1}}$.

The ADCP has a false target threshold built in which describes the maximum tolerated amplitude difference among the beams. If for example due to a fish passing one beams reading exceeds the threshold relative to the other, this beam is taken out of consideration and the velocity is computed with the remaining three beams. If more beams are corrupted, the data from the corresponding cell is rejected. Here, the default setting of 50 counts was used as threshold. With its fourth beam the Workhorse ADCP calculates the velocity error and rejects data with too high errors, here the default threshold of 2000 $\mathrm{mm\,s^{-1}}$ was kept. (*WorkHorse: Monitor, Sentinel, Mariner, Long Ranger, and QuarterMaster - Commands and Output Data Format* 2019)

WinSC was also used to download the data after each deployment. To view and export the data the software WINADCP Version 1.0.5 by RD Instruments (San Diego, USA) was used.

3.2. Lagoons

The currents in six testing sites in the lagoons and backwater channels (Figure 3.1) were profiled over the course of roughly three days per site with an Aquadopp Profiler 2 MHz Version 1.08 HR from Nortek (Rud, Norway). The ADCP was deployed downward-facing through a hole in the middle of a surfboard with the head, hold by a plastic clamp, hanging 4 - 5 cm below the water surface. The surfboard was secured with two or, if possible and necessary, four 6 m long ropes attached to adjacent mangrove trees and additionally stabilized by four PVC-pipes that allowed the surfboard to move vertically with the tides but restricted horizontal rotations and translations. All the materials used were non-magnetic. Programming was carried out with the AquaProHR High Resolution software Version 1.11.03 from Nortek (Rud, Norway). The ADCP was measuring for 1 second every minute with a frequency of 2 MHz, the compass updated every second. The cell size was 0.1 m with a blanking space of 0.15 m, the salinity fixed to 45 ppt. The ADCP was programmed with a pulse distance 0.1 m greater than the expected depth (Table A.2). Additionally the salinity for each deployment was taken as a single point measurement with a HI 98192 from Hanna Instruments Inc. (Woonsocket, Rhode Island).

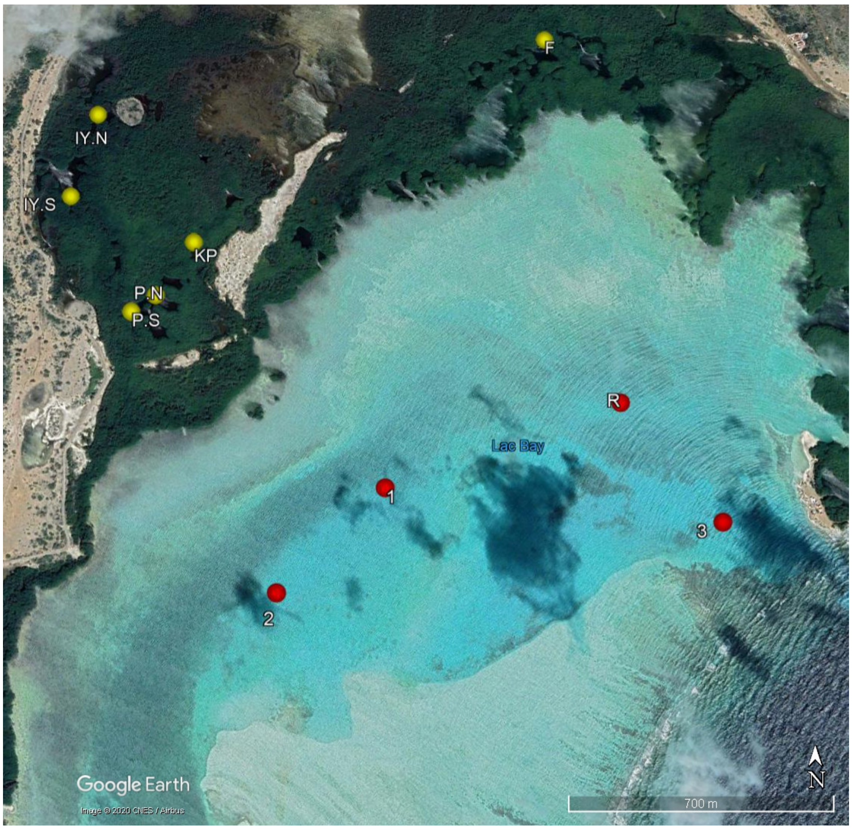

Site	Coordinates	Depth [m]
1	N12°06.223’ W68°13.984’	4.6 - 4.9
2	N12°06.066’ W68°14.156’	4.1 - 4.3
3	N12°06.171’ W68°13.471’	5.4 - 5.9
R	N12°06.355’ W68°13.609’	3.8 - 4.2
P.S	N12°06.500’ W68°14.374’	0.97 - 1.14
P.N	N12°06.527’ W68°14.335’	1.03 - 0.98
KP	N12°06.615’ W68°14.273’	0.94 - 0.98
IY.S	N12°06.693’ W68°14.472’	1.19 - 1.18
IY.N	N12°06.835’ W68°14.428’	0.88 - 0.92
F	N12°06.970’ W68°13.678’	1.68 - 1.41

Figure 3.1: Measurement locations for the ADCPs in the open part of Lac Bay (red, 1, 2, 3, R = Reference) and in the backwater area (yellow, P.S / P.N = Pedro South / north, KP = Kuki Perdi, IY.S / IY.N = Isla Yuwana South / north, F = Fogon), as well as coordinates and depths measured with a reel at deployment and retrieval for the measurement sites

3.3. Data processing for open bay and lagoons

All data for open bay and the lagoons was processed with RStudio Version 1.2.5001 (Boston, Massachusetts) with a few specifications necessary due to the different sensor types. Each beam for both types of ADCP was processed singularly instead of averaging in order to ensure the operability of each beam and the quality of the data.

Amplitudes lower than 15 counts above the noise floor of each beam were considered too noisy and were discarded. The noise floor for the Workhorse ADCPs was taken with the same configurations as the deployments (24 cells) over the course of 11 hours and the mean was taken for each beam. The noise floor for the Nortek ADCP was taken for each deployment with the deployment-specific range over 10 hours and averaged likewise. Since the amplitude of the returning signal is normally decreasing over a few cells, then increasing with range and peaking when the signal hits a barrier such as the surface or the bottom of the waterbody (Nortek AS 2018) the maximum amplitude was taken as the surface or the bottom and values after this maximum were discarded as well. The maximums were collected to give an overview over the deployments depth. Exceptions were made where the maximum was reported in unexpectedly early cells, which was interpreted as the surface or bottom laying beyond the range of the sensor. Therefore, amplitudes with a maximum within the first 3 cells in case of the Nortek ADCP and within 10 cells in case of the Workhorse ADCP were kept.
The correlation threshold for the Nortek ADCP was set to 70 %, data points below this percentage were discarded. The Workshorse ADCPs are scaling the correlation to 128 and outputting it in counts. The default is a threshold at 64 counts (*WorkHorse: Monitor, Sentinel, Mariner, Long Ranger, and QuarterMaster - Commands and Output Data Format* 2019), meaning 50 % (Gordon 1996), in post-processing the threshold was set to 90 counts, resulting in 70.3 %.
The Nortek ADCP also had a maximum horizontal and vertical velocity resolution specifically for each deployment (Nortek AS 2018) (Table A.2), measurements with an absolute value exceeding this threshold were also considered incorrect and therefore discarded. For the Nortek ADCP the velocity measurements of each deployment were additionally corrected based on the corresponding salinity measurement following Nortek AS (2018):

$$V_{corrected} = V_{measured}(\frac{C_{new}}{C_{measured}}) \tag{3.1}$$

whereby V is the corrected or respectively the measured velocity and C the new or respectively the measured speed of sound. The new speed of sound was calculated with an increase in the speed of sound of 1.2 $\mathrm{m\,s^{-1}}$ with 1 PSU alteration in salinity (Nortek AS 2017) based on the planned salinity. For the Workhorse ADCPs this was deemed unnecessary since the error is very small and the salinity throughout the bay was much more homogeneous than in the lagoons.
All velocity measurements were at least one beam showed either invalid amplitudes and/or inadequate correlations were discarded. The hourly mean of the magnitude and vertical velocity was taken for the Nortek ADCP, whereby hours and cells with discarded measurements were averaged with the remaining data. The directions α were transformed from degree into radian and the average $\overline{\alpha}$ build with a circular mean (R. Jammalamadaka and Sengupta 2001):

$$\overline{\alpha} = \arctan\left(\frac{\sum_{i=0}^{n}\sin(\alpha_i)}{\sum_{i=0}^{n}\cos(\alpha_i)}\right) = \arctan\left(\frac{S}{C}\right) = \begin{cases} \arctan\left(\frac{S}{C}\right) & C > 0, S \geq 0 \\ \left(\frac{\pi}{2}\right) & C = 0, S > 0 \\ \arctan\left(\frac{S}{C}\right) + \pi & C < 0 \\ \arctan\left(\frac{S}{C}\right) + 2\pi & C \geq 0, S < 0 \\ \text{undefined} & C = 0, S = 0 \end{cases} \tag{3.2}$$

The vertical velocity as well as the magnitude and direction of velocity in degree of the first whole tidal cycle for each deployment were then plotted with the interpolating spline() funtion over time. For the Workhorse ADCPs in the open bay model tides were build: Each starting from a big high tide the tidal amplitude data for all fully measured roughly 24/25-hour-long tide cycles were interpolated to depict the hourly tidal range and a mean was taken over each specific time point relative to the initial high tide from all tide cycles. Similar to that the ADCP-data was averaged starting from the hour in which the big high tide occurred within each 24-hour-tidal cycle, building a model tide out of 5 - 7 tidal cycles for the hourly measurements over the cells starting at high time. For the directions the circular mean according to Equation 3.2 was taken in a similar procedure. The magnitude, direction and vertical velocity of the model tides were plotted over hours using spline().

4. Results

4.1. Model tides

The model tides cycles follow two types of tidal cycle. Type I tidal cycles started with a high tide between 0.54 - 0.57 m, the low tide follows 9 - 10 hours later with a tidal amplitude ranging from 0.23 - 0.26 m. The tidal cycle concludes with a second high tide with a range from 0.55 - 0.56 m after 24 - 25 hours, the tidal range is therefore 0.29 m to 0.34 m. The model tides for the deployment 1.2, 2.1 and 3.2 are tidal cycles type I.

Type II tidal cycles are between 24.3 - 24.8 hours long and start with the initial high tide being 0.44 - 0.50 m. The first low tide occurs 6 - 9 hours later with a tidal amplitude of 0.37 - 0.39 m followed by another so-called little high tide 11 - 12 hours after the initial high tide ranging from 0.39 - 0.45 m. 16 - 19 hours after the beginning of the tidal cycle a second low tide with a range between 0.33 - 0.37 m occurs. The model tide concludes with a high tide from 0.46 - 0.53 m, the maximum tidal range is therefore 0.09- -0.19 m. Deployment 1.1, 2.2 and 3.1 as well as deployment 1.3 showed model tide cycles Type II.

4.2. Reference point

During all deployments at the reference point the measurements showed a depth of 3.5 - 4.1 m, mostly around 3.9 m. The wind was blowing westwards with 3 - 11 $\mathrm{m\,s^{-1}}$ (*windguru: Bonaire, Sint Eustatius and Saba - Lac Bay*). The vertical magnitudes are ranging from - 19.75 $\mathrm{mm\,s^{-1}}$ up to 30 $\mathrm{mm\,s^{-1}}$ underneath the surface. Often times above a range of 3.3 m the velocities are becoming stronger, up to 74.0 $\mathrm{mm\,s^{-1}}$. This phenomenon is also observed in the horizontal magnitudes which are increasing drastically over the first 2 - 3 surface cells, sometimes up to 401 $\mathrm{mm\,s^{-1}}$ and the directions which tend north- till westwards. Other than that, the magnitudes did not show a clear pattern over the deployments. Ranging from 29.6 - 72.6 $\mathrm{mm\,s^{-1}}$ to 80.0 - 114.7 $\mathrm{mm\,s^{-1}}$ over the deployments the magnitude below the surface is widespread, but neither for the incoming tide compared to the outgoing tide nor between the deployments or the tidal cycle types a tendency in magnitude was observed (as shown in Table A.3). The directions below the surface during the outgoing tide were varying from west-southwest to east and east-northeast to northwest over the deployments, during the incoming tide they are ranging from northeast to south without any clear pattern. These as all following directional statement are turning clockwise.

4.3. Location 1 - 3 in the open bay

The surface for all deployments at location 1 lay between 3.4 - 3.9 m above the sea floor. The vertical magnitudes for all deployments at location 1 underneath the surface range between - 12.3 - 22.4 $\mathrm{mm\,s^{-1}}$, the vertical magnitudes for the 2 to 3 surface cells are mostly higher than those of the rest of the water column.

Deployment 1.1 and 1.3 (both tidal cycle type II) started with currents moving overall north till southeast with a magnitude between 62.6 - 135.6 $\mathrm{mm\,s^{-1}}$ during the high tide. With the outgoing tide the currents tend to northeast till east-southeast at the low tide while the magnitude increase up to 70.4 - 146.4 $\mathrm{mm\,s^{-1}}$. The following incoming tide and high tide do not show any relevant changes. During the next outgoing tide until the low tide the currents are heading northeast to east with a magnitude decreased between 70.6 - 137.4 $\mathrm{mm\,s^{-1}}$. The second incoming tide tends towards northeast to north-northwest near the surface above 2.6 m from the sea floor, below a depth of 2.6 m the directions range from east-northeast to southeast, tending towards east near the sea floor. The magnitude over the hours is decreasing to 42.7 - 107.6 $\mathrm{mm\,s^{-1}}$. Deployment 1.2 during a tidal cycle type I starts mostly heading east-northeast to east-southeast with 52.4 - 97.8 $\mathrm{mm\,s^{-1}}$ at the high tide tending towards east at the surface and south on the ground. During the outgoing tide the currents shift towards east-northeast to east at the low tide with at first decreasing, than increasing magnitude up to 72.0 - 132.4 $\mathrm{mm\,s^{-1}}$ 1 hour before low tide. In the following incoming tide the currents are ranging mostly from north-northeast to southeast. The magnitude is first increasing up to 127.4 $\mathrm{mm\,s^{-1}}$. At the high tide the magnitude is decreased to 41.5 - 82.3 $\mathrm{mm\,s^{-1}}$, the directions from north-northeast to south-southeast with channels tending towards south 1.5 - 1.9 m and 2.7 m above the ground.

The deployments at location 2 are measuring a depth between 3.2 m and 3.6 m and vertical velocities from -14.5 - 18 $\mathrm{mm\,s^{-1}}$ with a tendency towards higher magnitudes at the surface.

The first high tide during deployment 2.1 (tidal cycle type I) and the outgoing tide are showing a tendency from north at the high tide towards east-southeast over the hours and northwards near the surface, eastwards near the sea floor with a magnitude bandwidth from 51.2 - 117.3 $mm\,s^{-1}$. The low tide is ranging from north-northeast to east with a magnitude from 53.2 - 96.0 $mm\,s^{-1}$. The following incoming tide is tending towards northwest at the surface while the water column near the sea floor is heading east-southeast, the magnitude is widening to 31.2 - 121.2 $mm\,s^{-1}$. At the high tide the directions are tending towards northeast to east with magnitudes between 36.0 - 82.3 $mm\,s^{-1}$. Deployment 2.2, during a tidal cycle type II, is overall showing a strong tendency towards north till west near the surface and towards east near the sea floor. Underneath 3.1 m the currents are shifting minimal during the first outgoing tide from north-northwest to east-northeast at the high tide to north to east at the low tide. The bandwidth is narrowing further during the incoming tide, reaching north to east-northeast at the high tide. From there the directions are becoming less focused again up to the low tide with currents towards west-northwest to east. Afterwards, the currents are shifting back towards north, ranging from north-northwest to east during the final high tide. The magnitude over the whole model tide is ranging from 40.5 - 143.8 $mm\,s^{-1}$ without showing any tendency over the cells, only during the second outgoing and second incoming tide a minimal increase is noted.

The depth at location 3 varies from 3.3 m to 4.2 m with vertical magnitudes between -12.4 $mm\,s^{-1}$ and 29.0 $mm\,s^{-1}$.

The directions during deployment 3.1 during a tidal cycle type II vary barely. During the high tide a small tendency towards south near the surface and south-southwest near the sea floor can be seen. With the outgoing tide the magnitude underneath the surface is decreasing from 145.0 - 202.4 $mm\,s^{-1}$ to 120.4 - 176.2 $mm\,s^{-1}$ at the low tide, the directions are tending minimal towards southwest at the low tide. During the incoming tide and the following high tide the range is changing slightly towards south-southwest near the surface and south near the sea floor with a magnitude up to 186.8 $mm\,s^{-1}$. During the outgoing tide and the next low tide the tendencies in direction are shifting again to south near the surface, south-southwest near the sea floor, the overall range in magnitude is widening to 117.6 - 212.4 $mm\,s^{-1}$. During the final incoming and high tide the directions are ranging from south to southwest, the magnitudes from 80.0 - 185.2 $mm\,s^{-1}$.

Deployment 3.2 during a tidal cycle type I starts with the currents towards east-southeast to south underneath 3.1 m above the sea floor and east-southeast to northwest above that range with a magnitude between 65.2 - 122.8 $mm\,s^{-1}$. During the outgoing tide the bandwidth is increasing at first and narrowing down to east-southeast to south-southeast with the magnitude decreasing to 61.0 - 137.2 $mm\,s^{-1}$ at the low tide. The incoming tide is also moving mostly towards east-southeast to south underneath 3.1 m with a tendency towards east over time and a magnitude from 51.4 - 127.4 $mm\,s^{-1}$. The high tide is moving with 65.4 – 153.0 $mm\,s^{-1}$ towards east to south-southeast underneath 3.1 m from the sea floor and southeast to south above 3.1 m.

4.4. Deployments in the lagoons and backwater channels

The vertical velocities at Pedro South (Figure 4.1) in the entrance of the lagoon (tidal cycle type II) are ranging from -6.5 - 3.9 $mm\,s^{-1}$, the site is mostly 0.80 m deep. During the first high tide till 4 hours afterwards the currents are mainly heading north till north-northeast. Only the first 0.2 m show a south-southwest till west-southwest current, these bottom layers are generally delayed in directional changes and show a drastic decline in magnitude. The magnitude above 0.2 m is dropping from a maximum of 282.5 mm s^{-1} to 34.8 mm s^{-1}. After 5 hours, the currents during the outgoing tide, the low tide and the following incoming tide are going completely south till southwest with a tendency towards south at the range 0.2 - 0.4 m above the ground. The magnitudes are increasing around the low tide up to 68.9 mm s^{-1}. At the following little high tide the currents in the channel 0.2 - 0.4 m above the ground are changing abruptly towards north / north-northeast. 1 hour afterwards this layer initiates another turn towards southwest, at the low tide 5 hours after the last high tide the whole water column is moving southwards till southwestwards. The magnitude during the high tide and the first hour afterwards is ranging from 9.0 - 130.7 mm s^{-1}. For the next 4 hours the direction of the current is ranging from south to west-southwest with a decreased magnitude between 13.4 - 57.1 mm s^{-1}. 5 hours after the last low tide during the incoming tide the main currents are turning towards north / north-northeast, with the magnitude increasing up to 268.1 mm s^{-1}.

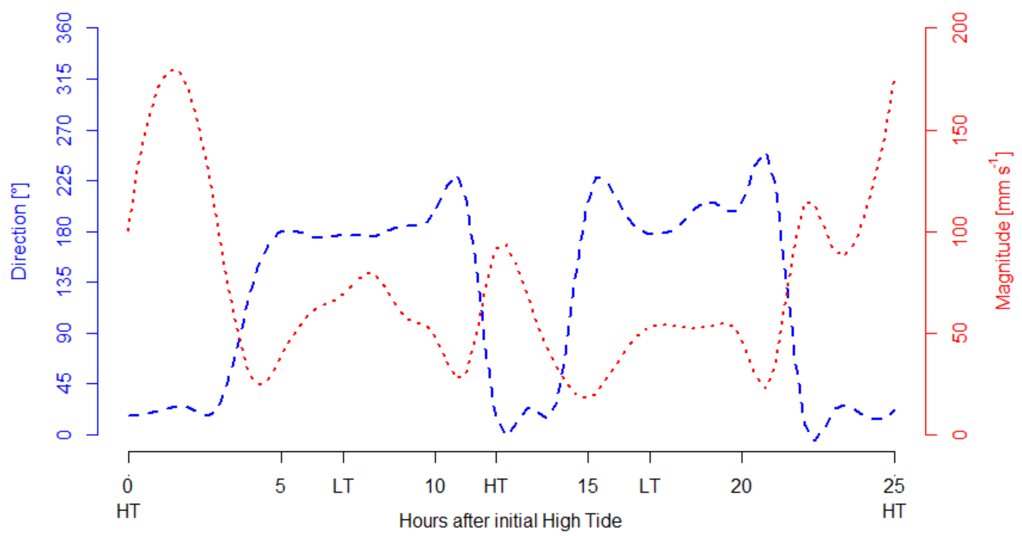

Figure 4.1: Directions (blue, dashed line) and magnitudes (red, dotted line) over one tidal cycle with the high tides (HT) and low tides (LT) at Pedro South 0.3 - 0.4 m above the ground.

Pedro North at the exit of the lagoon towards Kuki Perdi (tidal cycle type I), was 0.94 m deep during most of the incoming tide and 1.04 m around the high tide. The vertical magnitudes are ranging between - 4.2 mm - 4.0 mm s^{-1}. Starting with the high tide the currents are moving towards north-northwest till northeast. The magnitudes are ranging from 49.4 mm s^{-1} at the surface down to 0.5 mm s^{-1} at the bottom with 24.5 - 25 mm s^{-1} at 0.2 - 0.5 m (Figure 4.2). 1 hour afterwards the directions widen, the magnitudes decrease to 21.9 mm s^{-1} at maximum. From 2 hours after the initial high tide till the low tide 9 hours afterwards the currents above 0.1 m are moving south till southwest with a narrowing bandwidth over the hours and a tendency towards south with increasing depth. Initiated from 0.35 m above the ground the magnitude is rising from a maximum of 45.5 mm s^{-1} to 154.7 mm s^{-1} at the low tide. Till 6 hours after the low tide the magnitude is decreasing till 91.4 mm s^{-1} with its maximum still at 0.35 m above the ground and the edges of the water column ranging from south-southeast to west-northwest. After adjustment period of an hour, 8 hours after the low tide till into the next high tide the currents are heading mostly towards north-northwest till east-northeast, the magnitude dropped to a maximum of 33.2 mm s^{-1}.

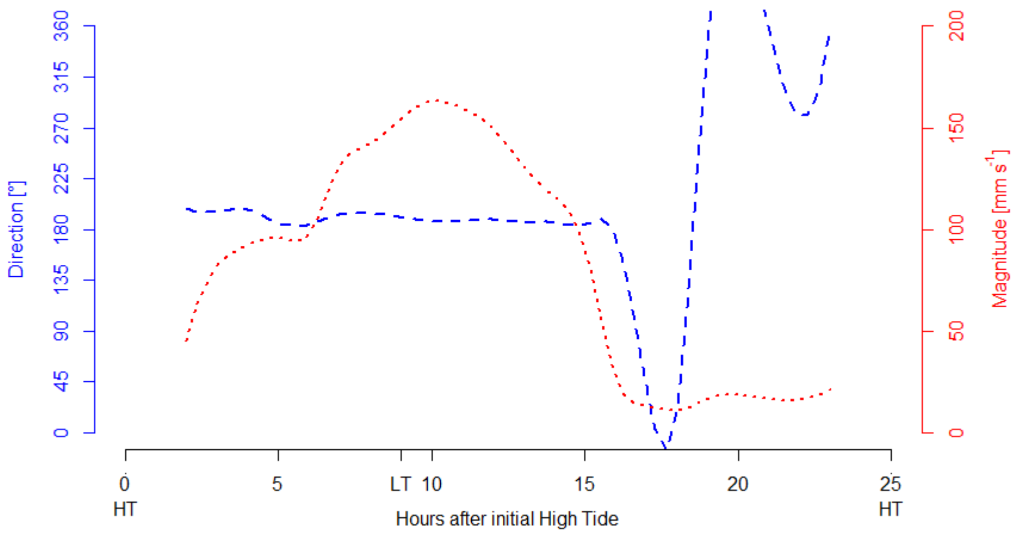

Figure 4.2: Directions (blue, dashed line) and magnitudes (red, dotted line) over one tidal cycle with the high tides (HT) and low tide (LT) at Pedro North 0.3 - 0.4 m above the ground.

The deployment in the lagoon Kuki Perdi during a tidal cycle type I varies in depth between 0.84 m and 0.94 m around the high tide. The vertical magnitudes are ranging from - 7.4 mm - 2.5 mm s^{-1} and are decreasing with depth. The measurements are showing a boundary layer of 0.1 - 0.2 m towards the ground. The initial high tide and the first two hours of the incoming tide are showing a tendency towards north / north-northeast and a magnitude between 36.5 - 122.1 mm s^{-1} above the range 0.5 m, underneath the currents are ranging from northeast till north including south-components with a magnitude up to 25.3 mm s^{-1} (Figure 4.3). After 4 hours the directions above 0.1 m are becoming steady heading south-southeast till south-southwest until the low tide, tending towards west 0.3 - 0.5 m above the ground with magnitudes up to 41.3 mm s^{-1}. During the first 8 hours of the incoming tide the bandwidth of the directions is widening to mostly southeast till west-northwest with a tendency towards east within the channel 0.2 - 0.4 m above the ground and towards west on the edges of the water column. Meanwhile the magnitude above 0.1 m is decreasing over the hours from 27.9 - 39.9 mm s^{-1} to 1.1 - 26.2 mm s^{-1} with a tendency towards higher magnitudes at the surface. After 8 hours the directions are beginning to change eastwards starting at 0.35 m, 10 hours after the low tide the currents above 0.3 m are ranging from north-northwest till north-northeast with an increasing tendency towards north advancing the high tide. The cells underneath 0.4 m are following slowly and the magnitudes are increasing again. At the high tide the directions are ranging from north to northwest with magnitudes up to 134.7 mm s^{-1} at the surface.

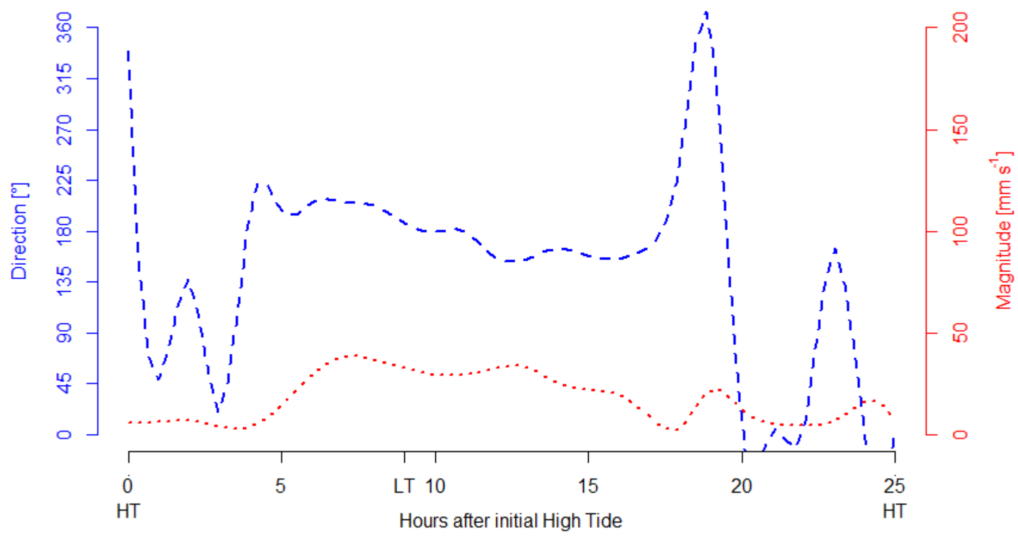

Figure 4.3: Directions (blue, dashed line) and magnitudes (red, dotted line) over one tidal cycle with the high tides (HT) and low tide (LT) at Kuki Perdi 0.3 - 0.4 m above the ground.

The measurement at Isla Yuwana South in the entrance of the lagoon during a tidal cycle type II is showing a water depth of 1.09 m. The vertical magnitudes are ranging from - 2.9 - 2.0 $\mathrm{mm\,s^{-1}}$ whereby the water column near the surface tends to move downwards.

The directions during the first high tide are heading northeast below 0.2 m and ranging from southeast to south-southwest above 0.2 m from the ground. Till 3 hours after the high tide the directions are barely changing, ranging from southeast to southwest. The magnitude is ranging from 3.6 $\mathrm{mm\,s^{-1}}$ up to 21.1 $\mathrm{mm\,s^{-1}}$ at the surface. 4 hours after the high tide till an hour before the next high tide the currents within up to 0.5 m above the ground are moving occasionally towards north till east but the overall direction is south-southeast till west. The magnitude is barely changing, ranging from 3.6 - 17.4 $\mathrm{mm\,s^{-1}}$ with a decrease over depth. During the second high tide till 2 hours afterwards the currents above 0.3 m are moving northwest till east-northeast tending northwards over the hours while the magnitude pattern remains mostly identical. The rest of the outgoing tide as well as the low tide is characterized by southeast till southwest heading current with a tendency towards west over the hours and within the range 0.2 m up to 0.4 m above the ground, shown in Figure 4.4. The magnitude is slightly increasing. This trend continues over the incoming tide until the currents are moving mainly northwards during the high tide, the magnitude is overall increasing up to 35.4 $\mathrm{mm\,s^{-1}}$.

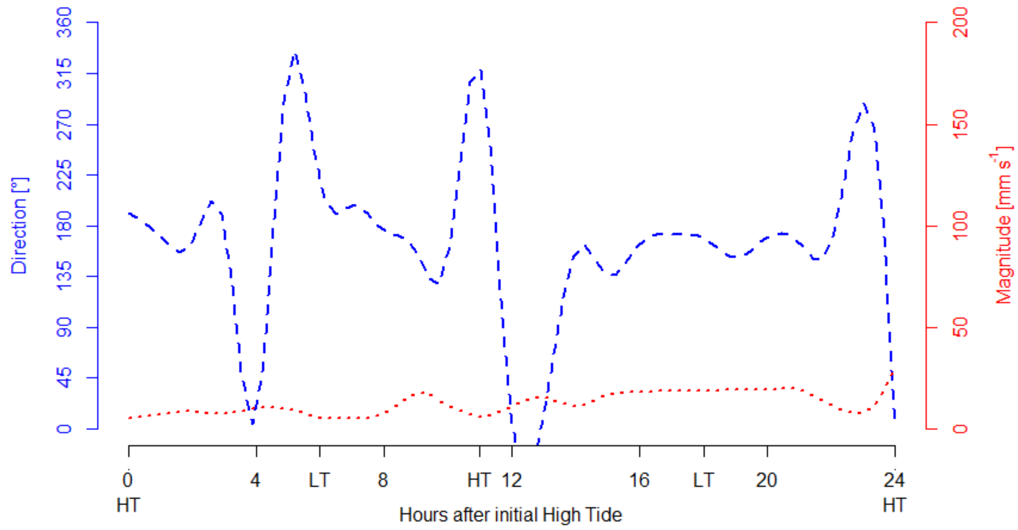

Figure 4.4: Directions (blue, dashed line) and magnitudes (red, dotted line) over one tidal cycle with the high tides (HT) and low tides (LT) at Isla Yuwana South 0.3 - 0.4 m above the ground.

The deployment Isla Yuwana North, in a 0.83 m deep channel between two lagoons during a tidal cycle type II showed severely dropping velocity magnitudes for the last 0.1 m above the ground. Therefore the following is narrowed down to the data above this boundary layer. The vertical velocities are ranging mostly from - 3.7 - 3.7 mm s^{-1}.

The directions during the initial high tide are ranging from south-southwest to west-southwest with a tendency towards west with increasing depth. The magnitude is decreasing with depth from 51.7 mm s^{-1} to 27.7 mm s^{-1}. 2 - 3 hours into outgoing tide the directions underneath 0.4 m from the ground are turning towards north-northeast till east-northeast (Figure 4.5) for a moment, but 4 hours after the high tide and during the following low tide the directions are going towards southwest till west-southwest again. The magnitudes are ranging from 9.8 - 33.1 mm s^{-1}, during the change in directions the maximum magnitude is shifting from the surface to 0.2 -0.4 m above the ground. At the beginning of the incoming tide the directional range remains the same, with maximum magnitudes 0.2 -0.4 m above the ground. Starting 3 hours after the low tide from the ground the currents are turning, heading increasingly throughout the water column towards northeast to east-northeast. The magnitude, ranging from 9.4 - 38.9 mm s^{-1}, is not showing a tendency over the hours but maxima around 0.2 - 0.4 m above the ground. At high tide the currents are moving completely towards east with a magnitude from 45.4 - 61.8 mm s^{-1} peaking 0.25 m above the ground. With the beginning outgoing tide the directions are shifting slightly towards east-northeast and decreasing in magnitude. 4 hours after the last high tide the current is turning again towards south-southwest till west-southwest and the maximum magnitude is shifting towards the surface. During the following incoming tide and high tide the currents are heading increasingly towards south-southwest till west-southwest with a magnitude increasing up to 72.6 mm s^{-1} at 0.2 - 0.4 m above the ground.

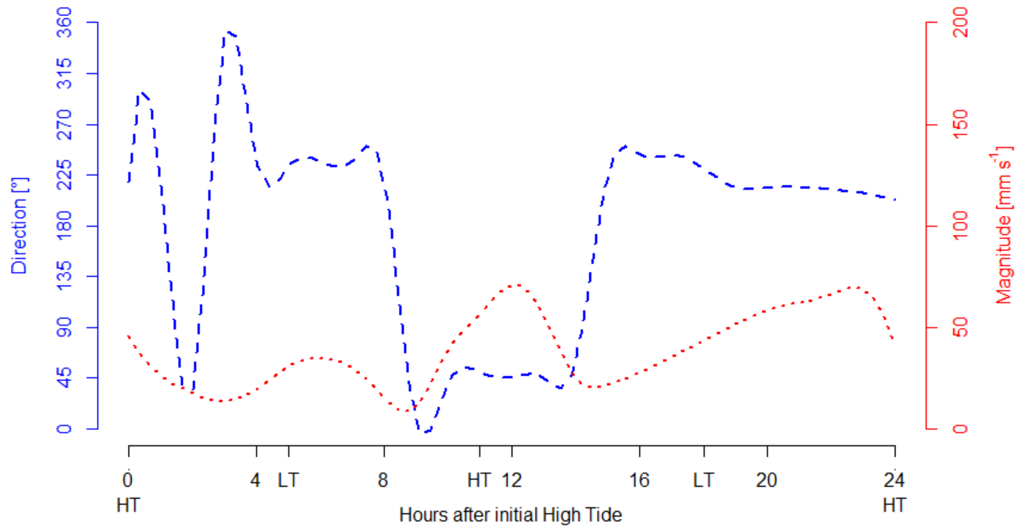

Figure 4.5: Directions (blue, dashed line) and magnitudes (red, dotted line) over one tidal cycle with the high tides (HT) and low tides (LT) at Isla Yuwana North 0.3 - 0.4 m above the ground.

The deployment in Fogon (Figure 4.6) during a tidal cycle type II measured depths between 1.34 m around the second low tide and 1.54 m around the big high tides and vertical velocities from -1.5 - 0.9 $mm\,s^{-1}$. At the initial high tide the directions above 0.4 m are ranging from north to east-northeast with magnitudes up to 31.0 $mm\,s^{-1}$ and from southwest to west with magnitudes from 4.1 - 4.3 $mm\,s^{-1}$ below 0.4 m from the ground. During the outgoing tide the main direction is southeast to west-southwest tending towards east over the hours, the magnitude is ranging from 1.4 $mm\,s^{-1}$ underneath 0.4 m up to 36.7 $mm\,s^{-1}$ near the surface. During the low tide the currents are widening up to north-northwest to east-northeast near the surface, east-southeast to west in the middle and northwest near the ground while the magnitude is dropping to 1.5 $mm\,s^{-1}$ at maximum.

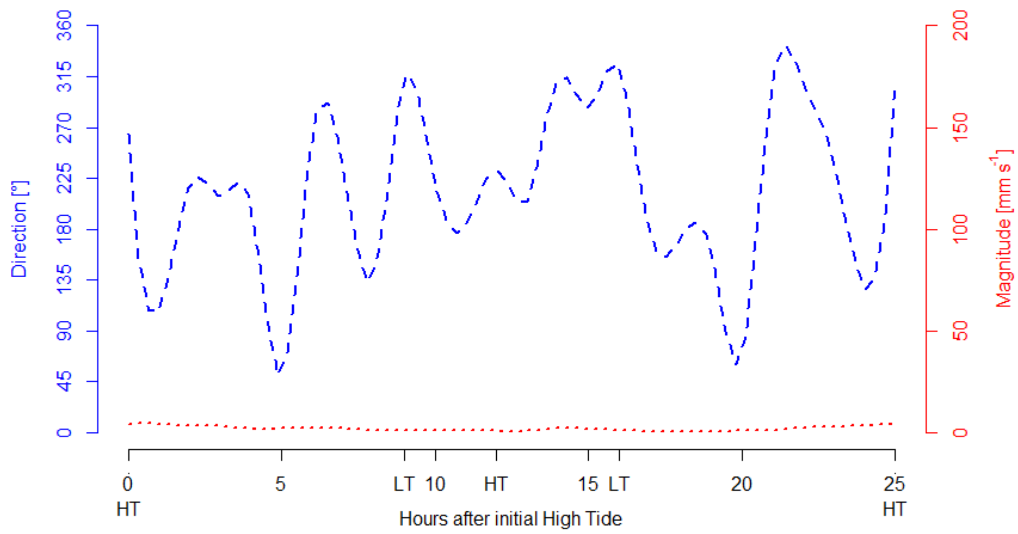

Figure 4.6: Directions (blue, dashed line) and magnitudes (red, dotted line) over one tidal cycle with the high tides (HT) and low tides (LT) at Fogon 0.3 - 0.4 m above the ground.

The currents are becoming more focused again 2 hours after the second low tide. Beginning with range 0.55 m the currents are tending westward, ranging from west-northwest to east-northeast at the high tide. The magnitude is increasing up to 33.5 $\mathrm{mm\,s^{-1}}$.

5. Discussion

5.1. Reference point and methodology

As shown in subsection 4.2 the currents at the reference point throughout the whole water column do not seem to follow the tides clearly. However, the currents during the incoming tides seem to have an overall slightly more eastward tendency and the outgoing tide a minimal tendency towards south. There is no general change in magnitude with the currents, generally the range between incoming and outgoing tide over one deployment is relatively small, probably due to the relatively small tidal range with a maximum from 0.34 m. The magnitudes here are overall smaller than the ones measured at other sites. Also, no apparent tendency from tidal cycle type I to tidal cycle type II can be shown. All this is a much more chaotic behavior than expected, which also means the value of this location as a reference point is to be viewed critically. Although the reference point was chosen to be in the middle of the bay towards the exit, in light of the results it seems a more eccentric position would have maybe allowed for clearer tidal directional changes and therefore given more reliable data regarding the temporal changes in the currents over the deployments. Nevertheless, the single deployments can be considered time-independent since the reference point did not show any shift in direction or magnitude over the deployments.

5.2. Open bay

Throughout all deployments in the open bay (including the reference point) the data shows extremely high horizontal and vertical magnitudes for the first one to three cells at the surface, whereas the effect is much stronger at the reference point and location 3, which are closer to the exit than those further in the relatively protected bay. The directions within these cells generally fit the constantly westwards blowing wind without changing with the tides and are therefore to be seen as edge layer. The measurements during a tide type II are, at all deployments, very unclear from the first little low tide till the second little low tide. Obviously, the system does not have enough time to react properly to those often only 3 hours consecutively following tides with tidal ranges under 0.1 m. Usually, even with high tidal ranges at the beginning and end of tidal cycles type II and during tidal cycles type I, the directions and magnitudes are still very widespread for at least an hour, till the water body fully reacts to the tidal change.

Overall, the currents at location 1 are heading towards northeast to southeast during the incoming and east-northeast till east during the outgoing tide. The general tendency towards south for the incoming and those towards east for the outgoing tide are more distinct during the deployment with a tide type I with much higher tidal ranges and more time for the system to react. Also, the incoming tide shows a clear distinction between the below surface currents below the direct influence of waves and wind which are heading northeast and the deeper currents which are heading southeast. This shows the incoming tide pressing into the bay over the coral reef similar to Moorsel and Meijer (1993) and from the upper parts of the opening, while the bottom layers are still moving towards the exit. This explains why the outgoing tides move at higher velocities than the incoming ones; Basically, the movement in one direction throughout the water column at the outgoing tide allows higher velocities than the contrasting currents during the incoming tide. All in all these findings show similar results as Moorsel and Meijer (1993) in the below surface currents of the incoming tide but add a better understanding of the deeper layers.

The currents in location 2 seem to be less influenced by the tide, the changes in magnitude and a less clear pattern over the tides, as do the directions, which contrarily to Moorsel and Meijer (1993) are shifting a little from eastwards during the outgoing to northwards during the incoming tide. The smaller tendencies here are most likely due to the protected site in the middle of the bay, with greater distance to the exit and nearer to the coral reef, which prevents the water from exiting during the outgoing tide. Therefore, the bottom layers here are still moving mostly east without regard to the tides, while the surface is tending north- till westwards. The differences between these findings and the previous study (Moorsel and Meijer 1993) could be attributed to the loss of the 1993 existing mangroves nearby and the damage Hurricane Ivan caused to the reef in 2004 (Engel 2008).

Location 3 -similar to the reference point- is showing an all in all very unclear current which barely seem to follow the tides instead of showing a distinctive exiting and entering current may be expected from a position so close to the opening: While the outgoing tide is meeting the expectations of a east-southeast (towards the exit) heading current, the directions for the incoming tide are changing barely. The most likely explanation are turbulences due to the near coral reef as well as this being the area where the incoming tide is mixing with the seemingly continuous stream of outgoing current in the bottom. The map created by Moorsel and Meijer (1993) supports this theory, showing a underlying outgoing stream.

5.3. Backwater channels and lagoons

The deployment in Pedro South (tidal cycle type II), the one nearest to the open bay, is showing how the current needs 3 - 4 hours after the big high tide till it follows the tide outside completely. Altough the delays are shorter for the little tides with small tidal ranges which follow shortly onto each other, they are much longer than the 35 minutes Moorsel and Meijer (1993) measured as delay for the high tide an a spot a little further south. One reason could be that high tide does not mean complete turn in the currents, another the expansion of the mangroves into the open bay which elongated the Pedro channel drastically. The fact that Moorsel and Meijer (1993) also measured a tidal amplitude of 0.36 m whereas nothing of the sort was measured with the ADCP supports this explanation. This long delay easily explains the chaotic and often times seemingly unfitting currents during the little tides. All in all the incoming tide leading to north to north-northeast heading current and the outgoing tide leading to south till southwest heading current is matching the expectations but showing the influence of the northern laying lagoon in the bandwidth of the directions of the outgoing currents. The change towards a south-southwest current during the incoming tide is initiated from the ground layer, which suggests that contrary to the open bay, were the channel is showing an ongoing outwards stream even during high tide, the much shallower backwater channel and lagoon system is working the other way around with remains of the outgoing currents on the surface. The by Moorsel and Meijer (1993) observed exchange at the two opening towards the bay is not relevant anymore since the channel advanced much further and the second arm has grown shut.

During the deployment in Pedro North during a tidal cycle type I the currents are more homogeneous over the cells, maybe due to the relatively large lagoons in both directions serving as buffer storage. While the directions (north to east-northeast during the incoming, south-southwest during the outgoing tide) are expected, this could explain the drastic increase of 466 % in magnitude for the outgoing tide in comparison to the incoming tide since the northern Lagoon Kuki is much smaller than the southern Pedro Lagoon, which the incoming tide has to pass. While the currents need 8 hours after the big low tide to turn fully with the incoming tide the outgoing tide, coming from a much smaller lagoon, needs an adjustment period of only 2 hours - this period is shorter than the one observed in Pedro 2 which lies closer towards the bay, most likely due to the longer tides and higher tidal range during this deployment. The difference in delay time from incoming to outgoing tide not only supports the role of the lagoons buffering the incoming tide but also fits the sheet flow over the mangroves described in Wosten (2013) with the incoming tide pressing in over the whole boundary and the outgoing tide collecting the joined amount of water over the whole area into the channels. As expected all locations show a the boundary layer towards the ground with magnitudes dropping down to nearly 0 $\mathrm{mm\,s^{-1}}$ and greater directional delays. Here it is usually 0.3 m high and therefore more pronounced than at Pedro 2, suggesting the channel is filled with much more fine, colloid sediment. The directions for the incoming tide in Kuki Perdi during a tidal cycle type I are as expected south-southeast to south-southwest. The bandwidth is, as in Pedro 2, wider than in Pedro 1 - again due to the testing site in the middle of the lagoon. Interesting here is the over three times lower magnitude in comparison to the incoming tide, most likely because the ADCP was sitting right in front of the channel, fully absorbing the incoming current, which was accelerated by the narrow channel. The incoming tide is highly interesting to the decision for the placement of a new channel, as two options present itself: One oriented more towards west that would pass the western lagoons on its way towards the backwater area and one more straight forward to the north (Figure 2.1). Over the incoming tide as well as its adjustment period, eastern components are as well represented as northern components in amount and fewer western tendencies. The spatial distribution of these components is nevertheless remarkable: The surface layers tend to head more towards north while the bottom layer represent most of the westwards measurements. Since the surface layers are in general also showing higher magnitudes, a channel serving those currents would probably be more beneficial. Also, with a wide opening into the lagoon, it could maybe allow for the western currents to at least partially be lead into the channel as well. Additionally to all that, the boundary layer at the bottom with 0.2 m suggests trapped sediment again. A channel could help flush this out into the bay, increasing the currents and therefore the water exchange even further.

While the delay in the outgoing tide at Isla Yuwana South (during a tidal cycle type II) is hard to define due to the little tides, the incoming tide is also showing a 4 hour delay and is therefore similar to the one in Kuki Perdi, probably because the current needs to travel further, but the channels are also more straight than to Kuki were the southern lagoon is deflecting. The measured delay here is assimilating to the still smaller delay of 2:35 hours measured by Moorsel and Meijer (1993), while instead of the former measured 0.155 m tidal range the ADCP is not picking up any changes in depth. All in all the directions shown during the incoming tide from southeast to southwest are relatively expected. The outgoing tide however is displaying an exceptionally large bandwidth in directions. One reason is surely the placement into the large lagoon which is deflecting the currents to its total bandwidth of 274 °, the western component could also be explained by the sheet flow which is probably directing a great amount of outgoing water from the large mangrove cover east to the lagoon into the same. Generally, the magnitude of the currents is much smaller here than at the previously described sites.

The deployment during a tidal cycle type II at Isla Yuwana North in a channel connecting two lagoons is showing a clearer pattern again, the tidal delay remains at 4 hours, still 0:51 hour higher than in Moorsel and Meijer (1993) and also without their observed tidal range of 0.15 m. While the mostly southwest till west-southwest outgoing current is matching the expectations, the incoming current with its main direction being northeast to east-northeast seems deflected, probably pressing into the mangroves surrounding the lagoon rather than the almost completely overgrown channel (Figure 2.1) towards north which would create a water exchange in this remote area. Considering the position within a channel the magnitudes are relatively low, which aggravates the problem of insufficient water income, showing why the backwater areas are becoming hypersaline (fittingly, the salinity measurement is the highest of all sites). Opening this channel could possibly do a great deal towards redirecting these currents into the northern lagoon.

The southeast till west-southwest currents measured during the outgoing tide of a tidal cycle type II at Fogon are suggesting the water is leaving the area towards the great Fogon lagoon southwest, similar to that, the currents heading west-northwest till east-northeast seem to enter from here during high tide instead of through the channels towards east (Figure 2.1) as maybe expected at first, although it would definitely require more measurement sites along the channel and into the southwestern lagoon in order to verify this theory; It is not excluded that the currents could simply be deflected and turbulent in the large lagoon.

Overall, all deployments showed distinctive channels initiating the changes during the tidal cycles in direction and magnitude, often leading to local maxima in magnitude during the incoming and outgoing tide. For the western measurement sites in general such a channel 0.3 - 0.4 m above the ground could be identified, sometimes the channel even ranges from 0.2 m to 0.5 m above the ground. Only Fogon with its much greater depth displays a similar channel at range 0.5 -0.6 m above the ground.

5.4. Conclusion

Overall it could be shown that the system inside the open bay and especially inside the backwater channels represent a sheet flow and that the system needs time to react to tidal changes, small tidal ranges or tides shortly following each other therefore lead to chaotic, oscillating currents without a real water exchange in the northern parts of the bay. Also, the bandwidth of the directions is increasing with distance to the open bay while the magnitude is in general decreasing, however it should be kept in mind that it is not possible to determine the actual water exchange in those areas without knowing the areas of the testing sites. One reason for this is the buffering and deflecting functions of the large lagoons, another the long, not always perfectly oriented channels. Recommendations for the realization of new channels were given in the hopes of optimizing the water income and flushing out hindering sediments with the outgoing tides.

6. Perspective

To fully understand the hydrodynamics additional testing sites especially in the open parts of the bay and the lagoons would be needed, ideally with a high-resolution ADCP such as the used Nortek to minimize the blanking space in the open parts of the bay as well. Also, measuring over the course of a year would be beneficial to show the seasonal tides which are changing throughout the year up to 0.3 m being the highest in February (Moorsel and Meijer 1993). Also, a follow up study after the opening of new channels would be highly interesting to determine the success of specific measures and further optimizing these efforts.
Given these further investigations a detailed knowledge about the connected fluxes in Lac Bay could not only help maintaining and increasing the health of the mangroves but also in managing the seasonal *Sargassum* hits which are threatening its vulnerable ecosystem. During *Sargassum* outbreaks this seaweed drifts from large seagrass beds upstream to Bonaire, is washed ashore and accumulates in large quantities on the beaches. This not only impacts the local tourism negatively but also kills the local seagrass beds and harm the bentic life by developing toxic sulfide when decomposing. Although this global phenomenon cannot be prevented locally, understanding the currents could hep predict how and were *Sargassum* will be drifting and hitting the shore, potentially allowing to warn affected regions earlier and more specifically and preparing for it, maybe even catching *Sargassum* while drifting before it accumulates on the shore. (Geest et al. 2019)

7. Sources

7.1. Literatur

Engel, MS (2008). "Results of Survey Lac Bay, Bonaire for Queen Conch (Strombus gigas) and Seagrass characterization in 2007". In: *Bonaire National Marine Park, Stinapa*.

Moorsel, GV and Meijer, M (1993). *Base-line ecological study van het Lac op Bonaire*. Vol. rapport nr. 92.22. Bureau Waardenburg.

R. Jammalamadaka, S and Sengupta, A (2001). "Topics in circular statistics". In: Series on multivariate analysis, v. 5. xi, 322. World Scientific. Chap. Chapter 1 - Introduction, pp. 1 –24.

7.2. Additional sources

Davaasuren, N and Meesters, EH (2012). *Extent and health of mangroves in Lac Bay Bonaire using satellite data*. Tech. rep.

Debrot, AO (2012). *Baseline survey of anthropogenic pressures for the Lac Bay ecosystem, Bonaire*. Tech. rep. Den Helder.

Debrot, AO, Meesters, HWG, Leon, Ld, and Slijkerman, DME (2010). *Lac Bonaire - Restoration Action Spear Points, September 2010*. Tech. rep. Den Helder.

Engel, MS (2019). "Presentatie materiaal kanalen June 2019".

Geest, M Van der, Slijkerman, D, Mücher, C, Debrot, A, Burg, S, Teles, I, Henkens, R, Ghasemi, N, Kramer, H, Meijninger, W, and Lotz, B (2019). *Nexus interventions for small tropical islands: case study Bonaire (compilation of fact sheets 1 to 8)*.

Gordon, RL (1996). *Acoustic Doppler Current Profiler: Principles of Operation - A Practical Primer*. P/N 951-6069-00. RD Instruments.

Nortek AS (2017). *Nortek Manuals - Principles of Operation: 55 | 250 | 500 | 1000kHz*. N3015-009.

– (2018). *Nortek Manuals - The Comprehensive Manual for ADCP's: AWAC | Aquadopp | Aquadopp deepwater | Aquadopp Profiler | Aquadopp Profiler Z-cell | 2D Horizontal Profiler*. N3015-031.

RD Instruments (2001). *WorkHorse Sentinel ADCP User's Guide*. P/N 957-6163-00.

Tourism Bonaire. Last viewed: 29.01.2020. URL: `https://www.tourismbonaire.com/`.

windguru: Bonaire, Sint Eustatius and Saba - Lac Bay. Last viewed: 16.01.2020. URL: `https://www.windguru.cz/`.

WorkHorse: Monitor, Sentinel, Mariner, Long Ranger, and QuarterMaster - Commands and Output Data Format (2019). P/N 957-6156-00.

Wosten, JHM (2013). *Ecological rehabilitation of Lac Bonaire by wise management of water and sediments*. Tech. rep. Wageningen.

A. Appendix

A.1. Additional deployment details

Table A.1: Details of the measurements in the open bay: The distribution of the surroundings between sand and seagrass on a percentage basis, the start and end date and time in 2019 for each deployment whereby the reference deployments are identical with the corresponding deployments throughout location 1 - 3 as well as the measured depth from the surface to the head of the ADCP and the sea floor at deployment and retrieval.

Location	1			2		3		R						
Seagrass [%]	30			0		5		90						
Sand [%]	70			100		95		10						
Round	1.1	1.2	1.3	2.1	2.2	3.1	3.2	1.1	1.2	1.3	2.1	2.2	3.1	3.2
Deployment														
Time	25.09., 09:00	16.10., 09:30	06.11., 08:30	02.10., 10:00	23.10., 09:00	08.10., 09:30	30.10., 09:30							
Distance surface to ADCP [m]	4.5	4.5	4.6	4.0	4.0	5.2	5.6	3.7	3.7	3.6	3.9	3.6	3.6	4.0
Distance surface to sea floor [m]	4.7	4.6	4.8	4.2	4.2	5.4	5.9	4.0	3.9	3.9	4.0	3.8	3.8	4.2
Retrieval														
Time	02.10., 08:00	22.10., 09:00	13.11., 14:30	08.10., 09:00	29.10., 09:00	15.10., 08:00	05.11., 09:00							
Distance surface to ADCP [m]	4.6	4.7	4.8	4.0	4.1	5.6	5.4	3.8	3.8	3.8	3.8	3.8	3.8	3.7
Distance surface to sea floor [m]	4.7	4.9	5.0	4.1	4.3	5.8	5.7	4.0	4.0	4.1	4.0	4.0	4.0	3.9

Table A.2: Details of the measurements in the channels and lagoons: The measured salinity and the beforehand expected depth as basis for the ADCP pulse distance and cell number, from which the maximal horizontal and vertical velocity ranges are resulting. Additionally, the start and end date and time in 2019 for each deployment as well as the measured depth from the surface to the head of the ADCP and the overall depth at deployment and retrieval.

Location	Isla Yuwana South	Isla Yuwana North	Pedro North	Pedro South	Kuki Perdi	Fogon
Salinity [ppm]	47.2	50.4	46.1	43.6	46.2	38.6
Planned depth [m]	1.1	0.9	1.1	0.9	1.1	1.6
Number of cells	9	7	9	7	9	14
ADCP pulse distance [m]	1.2	1.0	1.2	1.0	1.2	1.7
Horizontal velocity range [$\mathrm{mm\,s^{-1}}$]	0.25	0.30	0.25	0.30	0.25	0.18
Vertical velocity range [$\mathrm{mm\,s^{-1}}$]	0.11	0.13	0.11	0.13	0.11	0.08
Deployment						
Time	06.11., 11:30	23.10., 11:30	02.11., 12:30	26.10., 10:30	30.10., 13:30	09.11., 18:30
Distance ground to ADCP [m]	1.15	0.83	0.99	0.92	0.9	1.6
Distance ADCP head to surface [m]	0.04	0.05	0.04	0.05	0.04	0.08
Retrieval						
Time	09.11., 11:30	26.10., 07:30	05.11., 08:30	29.10., 08:30	02.11., 10:30	13.11., 13:30
Distance ground to ADCP [m]	1.14	0.87	0.94	1.09	0.94	1.37
Distance ADCP head to surface [m]	0.04	0.08	0.04	0.05	0.04	0.04

A.2. Additional measurement data

Table A.3: Overview of the below-surface directions and magnitudes for the reference point in the open bay

Deployment	Tide type	Main Direction [°]		Main Magnitude [$\mathrm{mm\,s^{-1}}$]	
		Outgoing tide	Incoming tide	Outgoing tide	Incoming tide
1.1	2	E - S	ENE - S	31.6 - 80.8	45.2 - 81.8
1.2	1	E - NW, SE	NE - S	39.2 - 78.0	29.6 - 72.0
1.3	2	E - SE	E - SE	54.3 - 107.9	80.0 - 114.7
2.1	1	NNE - SE	NE - ESE	55.5 - 101.0	50.0 - 100.8
2.2	2	NE - ESE	NE - E	51.0 - 100.8	52.8 - 93.3
3.1	2	E - SSE	E - SE, SSW	59.4 - 103.0	59.8 - 100.8
3.2	1	NE - NW	NNW - SE	29.6 - 72.6	46.6 - 94.2

Acknowledgements

I would like to express my deep gratitude to my supervisor Dr. Lucy Gwen Gillis for making this project possible and supporting me greatly giving encouragement and criticism. My grateful thanks as well are extended to my supervisor M. Sabine Engel who was invaluable helpful in designing and carrying out the measurements in the field. I would also like to thank Jessica Jonker for all her support during the planning process and the field work. My gratitude also belongs to Gevelly Soliano for helping me with the deployments as well as the STINAPA and ZMT staff and all the volunteers including but not limited to Rens Jonker, Joost van Gaalen and Arno Verhoeven for their help during the field work. Thanks is also owed to Epiphane Yeyi for his help with the software and Johanna Aron for her input during writing. Last but not least I would like to thank Prof. Dr. Kesel for her patient support.

Declaration of authorship

Hereby, I declare that I have composed the presented paper independently on my own and without any other resources than the ones indicated. All thoughts taken directly or indirectly from external sources are properly denoted as such. This paper has neither been previously submitted to another authority nor has it been published yet.

Sophie Grützmacher,
Bremen, January 30, 2020

DAAD Deutscher Akademischer Austausch Dienst
German Academic Exchange Service

Erasmus+

ERASMUS+

Letter of confirmation for a placement abroad [SMP]

Academic Year 2018/19

It is hereby certified that

Mr./Ms. Grützmacher

home university ___**D Bremen 04**

has worked as a trainee in our institution

from 27/07/2019 **(day, month, year)**

to 16/11/2019 **(day, month, year).**

To be completed by the host institution:

STINAPA Bonaire **Name of host institution**

Peter Jager **Name of signatory**

Interim Director **Function**

November 16, 2019 **Date**

STINAPA BONAIRE
P.O. Box 368
Bonaire, C.N.
Tel.: (599) 717-8444 / 717-4163

Stamp and Signature

Please note that this certification should be filled in at the end of the student's stay abroad!

This letter of confirmation is usually replaced/complemented by a certified reference of traineeship from the host institution.